

# Single $\pi^0$ electro-production in the resonance region with CLAS\*

Kyungseon Joo<sup>1)</sup> (for the CLAS collaboration)

(University of Connecticut 2152 Hillside Road, Storrs, CT 06269, USA)  
(Universidad Técnica Federico Santa María, Valparaíso, Chile)

**Abstract** We report the analysis status of single  $\pi^0$  electroproduction in the resonance region to study the electromagnetic excitation of the nucleon resonances. The study is aimed at understanding of the internal structure and dynamics of the nucleon. The experiment was performed using an unpolarized cryogenic hydrogen target and 2.0 and 5.8 GeV polarized electron beam during the e1e and e1-6 run periods with CLAS at Jefferson Lab. The new measurements will produce a data base with high statistics and large kinematic coverage for the hadronic invariant mass ( $W$ ) up to 2.0 GeV in the momentum transfer ( $Q^2$ ) range of 0.3—6.0 GeV<sup>2</sup>. Preliminary results will be presented and compared with the various model calculations.

**Key words** nucleon resonances, electromagnetic transition form factors, nucleon structure

**PACS** 13.60.Le, 13.40.Gp, 14.20.Gk

## 1 Introduction

Electromagnetic excitation of nucleon resonances has been considered an important tool in understanding the complex nucleon structure. In particular, the transition amplitudes from the nucleon to its excited states are sensitive to the spatial and spin structure of the nucleon and are important for testing symmetry properties of the quark model<sup>[1, 2]</sup>. Pion electromagnetic production of pions has been investigated to study the excited states of the nucleon. The contributions from  $\pi^0p$  and  $\pi^+n$  channels account for nearly 90% of the meson electroproduction cross section in the resonance region.

A new generation of high precision photo- and electro-production experiments have now made it possible to measure both  $\pi^0p$  and  $\pi^+n$  channels with large kinematic coverage for the hadronic invariant mass ( $W$ ) and the momentum transfer ( $Q^2$ ). The most precise measurements exist for excitation energies around the  $\Delta(1232)$  resonance. Experiments using real photons at LEGS and Mainz and electrons at Bates, Bonn and Jefferson Lab have measured  $\Delta^+ \rightarrow p\pi^0$  decay angular distributions in or-

der to extract the form factors of the  $N\Delta$  transition amplitudes up to 6 GeV<sup>2</sup> in  $Q^2$ <sup>[3–5]</sup>. While new experimental data for  $\pi^+n$  channel are available up to 2 GeV in  $W$ <sup>[6, 7]</sup>, but lack of experimental data for  $\pi^0p$  channel above  $\Delta(1232)$  resonance region make a coupled channel analysis very difficult.

In this proceeding, we report the status of data analysis for  $\pi^0p$  channel, and preliminary results will be presented and compared with the various model calculations.

## 2 Experimental setup and event selection

The data were taken using the CEBAF Large Acceptance Spectrometer (CLAS) in Hall B at Jefferson Lab<sup>[8]</sup>. A schematic view of the CLAS is shown in Fig. 1. Six super-conducting coils generate 2 Tesla toroidal magnetic field pointing primarily along  $\phi$ . The space between the coils defines six wedge-shaped sectors which are individually instrumented as independent magnetic spectrometers. The detector package consists of drift chambers for charged-particle momentum reconstruction, gas Cerenkov counters for

Received 7 August 2009

\* Supported by U.S. Department of Energy, Office of Nuclear Physics, under Contract No. DE-FG-04ER41309 and in part through Contract No. DE-AC05-06OR23177, under which Jefferson Science Associates operates Jefferson Lab.

1) E-mail: kjoo@phys.uconn.edu

©2009 Chinese Physical Society and the Institute of High Energy Physics of the Chinese Academy of Sciences and the Institute of Modern Physics of the Chinese Academy of Sciences and IOP Publishing Ltd

$e/\pi$  separation, plastic scintillation counters for time-of-flight based particle identification, and sampling calorimeters to detect electromagnetic showers from electrons and photons.

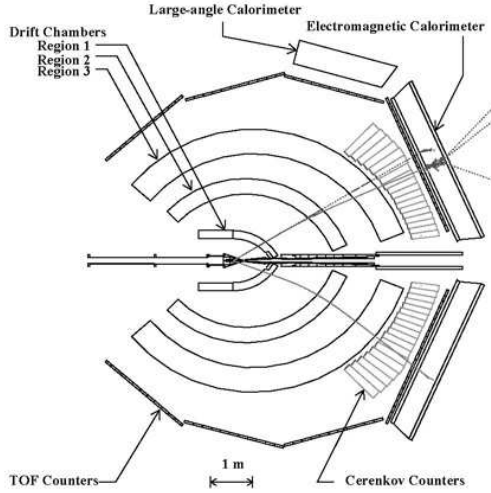


Fig. 1. Horizontal mid-plane cut through the CLAS detector at beam line elevation showing charged particles traversing the drift chambers (Region 1,2 and 3) in opposite sectors. Outside of Region 3 are time-of-flight (TOF) counters, calorimeters (EC), and Cerenkov counters (CC). The 2 Tesla toroidal magnetic field is contained within the boundary surrounding Region 2.

Beam electrons having energies of 2.445 GeV and 5.745 GeV were delivered at 100% duty factor onto a liquid hydrogen target at a current of 2.5 nA — 8 nA. Scattered electrons were detected over an angular range of  $20^\circ$  —  $55^\circ$  with a momentum resolution of  $\sigma_p/p \approx 0.5\%$  covering a range of  $Q^2 = 0.3$  —  $6.0$  GeV<sup>2</sup> and  $W$  up to 2.0 GeV. Coincident protons were identified by time-of-flight and exclusive  $\pi^0 p$  events identified using missing mass spectrum. Electron-proton co-planarity cuts were used to suppress the elastic Bethe-Heitler radiation as shown in as shown in Fig. 2. Target window backgrounds were suppressed with vertex cuts.

CLAS acceptance, tracking efficiency and resolution were simulated using a GEANT model of the detector geometry which incorporated the magnetic field map, surveyed positions of detector elements (including target position relative to coils), dead wires or TOF bars and measured wire chamber drift times. Software fiducial cuts were used to define the solid angle for electrons and protons, excluding regions of low Cerenkov efficiency or large multiple scattering from from magnetic coils. Proton energy loss in the target

and detector was included. Radiative correction is calculated using the approach of reference<sup>[9]</sup>, which is based on a covariant method for infrared cancellation is used, is used. Multiple soft photon radiation is included via exponentiation. This method is preferred over the Mo and Tsai procedure because (1) it addresses exclusive electroproduction rather than inclusive, (2) the infrared cancellation is independent of the unphysical parameter  $\Delta$  separating the phase space of soft and hard photons necessary in the Mo and Tsai procedure leading to uncertainties and (3) The approach of reference<sup>[9]</sup> does not rely on the peaking approximation, avoiding uncertainties at a few percent level associated with it. The large momentum and angular acceptance of CLAS permits events to be accumulated directly into bins of  $Q^2$ ,  $W$  and hadronic decay CM angles  $\theta_\pi^*$ ,  $\phi_\pi^*$ .

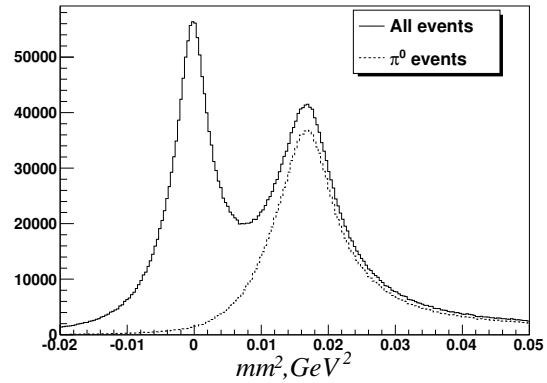


Fig. 2. Solid line: Missing mass squared spectrum ( $M_x^2$ ) from  $e + p \rightarrow e + p + X$  from E1E 2.445 GeV run. Dotted line: after the elastic Bethe-Heitler suppression.

### 3 Preliminary results

The exclusive pion electro-production cross section is given by:

$$\frac{d^3\sigma}{dQ^2 dW d\Omega_\pi^*} = J \Gamma_v \frac{d\sigma_u}{d\Omega_\pi^*}, \quad (1)$$

where  $J$ , the Jacobian and  $\Gamma_v$  is the virtual photon flux. For unpolarized beam and target, the differential cross section  $d\sigma_u$  depends on the longitudinal polarization  $\epsilon_L = (Q^2/|k^*|^2)\epsilon$  and transverse polarization  $\epsilon$  of the virtual photon through four structure functions,  $\sigma_T$ ,  $\sigma_L$  and their interference terms  $\sigma_{LT}$ ,  $\sigma_{TT}$ :

$$\frac{d\sigma_u}{d\Omega_\pi^*} = \frac{p_\pi^*}{k_y^*} (\sigma_T + \epsilon_L \sigma_L + \epsilon \sigma_{TT} \sin^2 \theta_\pi^* \cos 2\phi_\pi^* + \sqrt{\epsilon_L(\epsilon+1)} \sigma_{LT} \sin \theta_\pi^* \cos \phi_\pi^*), \quad (2)$$

where  $p_\pi^*$  and  $k_\gamma^*$  are the  $\pi^0$  momentum and photon energy in the CM frame, while  $|k^*|$  is the 3-momentum of the virtual photon. For a fixed beam energy, an out-of-plane measurement of the hadronic decay angles  $\theta_\pi^*$ ,  $\phi_\pi^*$  permits the separation of  $\sigma_T + \epsilon_L \sigma_L$ ,  $\sigma_{TT}$  and  $\sigma_{LT}$ .

Figure. 3 shows an example of the  $\phi_\pi^*$  dependence of the differential cross section compared with MAID2007 calculations. The structure functions  $\sigma_T + \epsilon_L \sigma_L$ ,  $\sigma_{TT}$  and  $\sigma_{LT}$  were extracted for each  $W$  and  $\cos\theta_\pi^*$  bin by fitting these data with the form

in Eq. (2). The solid line shows a typical fit. The  $\theta_\pi^*$  dependence of the extracted structure functions is shown in Fig. 4. Also shown are MAID2007 model calculations based on a fit to the previous world data using the Mainz Unitary Isobar Model (UIM). All errors shown throughout are statistical only. Absolute normalization uncertainty is around 5 %. Analysis of the full data set at multiple energies is underway, which will provide new data with a coverage up to  $Q^2 = 6.0 \text{ GeV}^2$  and  $W = 2.0 \text{ GeV}$ .

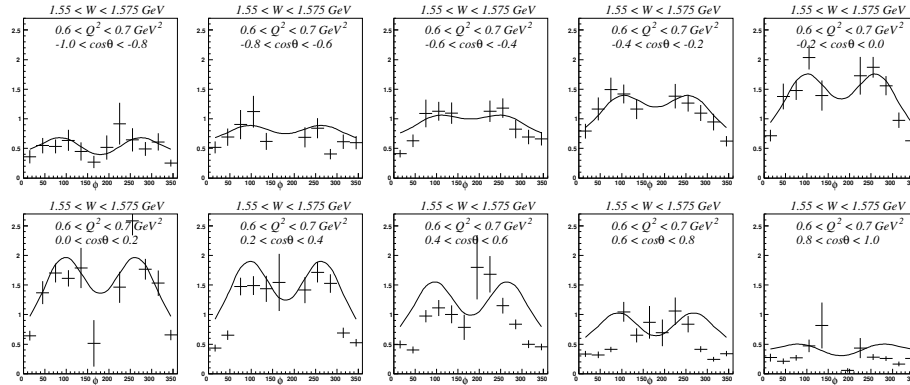


Fig. 3. Typical out-of-plane differential cross section at  $Q^2 = 0.65 \text{ GeV}^2$  and  $W = 1.565 \text{ GeV}$  for various  $\cos\theta_\pi^*$  bins. The solid line shows a typical fit. Statistical errors only.

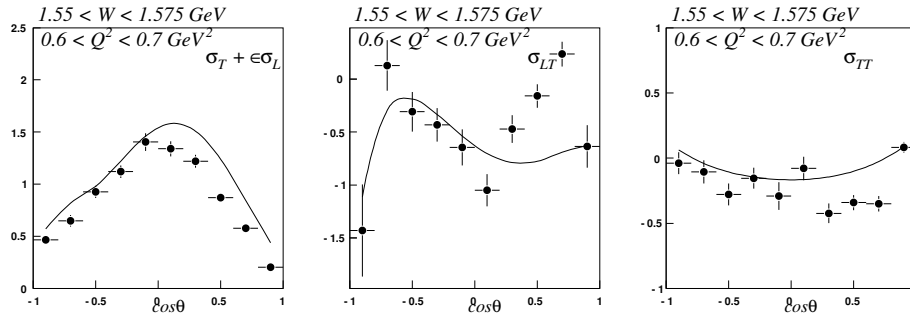


Fig. 4. Structure functions extracted at  $Q^2 = 0.65 \text{ GeV}^2$  and  $W = 1.565 \text{ GeV}$ . Solid line shows MAID2007 prediction. Statistical errors only.

## References

- 1 Isgur N, Karl G. Phys. Rev. D, 1978, **18**: 4187
- 2 Isgur N, Karl G. Phys. Rev. D, 1979, **19**: 2653
- 3 Frolov V V et al. Phys. Rev. Lett., 1999, **82**: 45—48
- 4 Joo K et al. Phys. Rev. Lett., 2002, **88**: 122001
- 5 Ungaro M et al. Phys. Rev. Lett., 2006, **97**: 112003
- 6 Park K et al. Phys. Rev. C, 2008, **77**: 015208
- 7 Egiyan H et al. Phys. Rev. C, 2006, **73**: 025203
- 8 Mecking B et al. Nucl. Inst. Meth. A, 2003, **503**: 513
- 9 Afansev A, Akushevich I, Burkert V D, Joo K. Phys. Rev. D, 2002, **66**: 074004